Follow us @BoneJointRes

Freely available online OPEN ACCESS

BJR

BONE BIOLOGY

LY3023414 inhibits both osteogenesis and osteoclastogenesis through the PI3K/Akt/GSK3 signalling pathway

X. Chen,
W. Chen,
Z. M. Aung,
W. Han,
Y. Zhang,
G. Chai

From Shanghai Ninth People's Hospital, Shanghai Jiao Tong University School of Medicine, Shanghai, China

Aims

LY3023414 is a novel oral phosphatidylinositol 3-kinase (PI3K)/mammalian target of rapamycin (mTOR) dual inhibitor designed for advanced cancers, for which a phase II clinical study was completed in March 2020; however, little is known about its effect on bone modelling/remodelling. In this study, we aimed to explore the function of LY3023414 in bone modelling/remodelling.

Methods

The function of LY3023414 was explored in the context of osteogenesis (bone formation by osteoblasts) and osteoclastogenesis (osteoclast formation and bone resorption). Murine pre-osteoblast MC3T3-E1 cell line and murine bone marrow-derived macrophage cells (BMMs) were subjected to different treatments. An MTS cell proliferation assay was used to examine the cytotoxicity. Thereafter, different induction conditions were applied, such as MCSF and RANKL for osteoclastogenesis and osteogenic media for osteogenesis. Specific staining, a bone resorption assay, and quantitative real-time polymerase chain reaction (qRT-PCR) were subsequently used to evaluate the effect of LY3023414. Moreover, small interfering RNA (siRNA) was applied to knockdown Akt1 or Akt2 for further validation. Lastly, western blot was used to examine the exact mechanism of action.

Results

LY3023414 attenuated PI3K/protein kinase B (Akt)/GSK3-dependent activation of β-catenin and nuclear factor-activated T cell 1 (NFATc1) during osteogenesis and osteoclastogenesis, respectively. LY3023414 mainly inhibited osteoclast formation instead of mature osteoclast function. Moreover, it suppressed osteogenesis both in the early stage of differentiation and late stage of calcification. Similarly, gene knockdown of Akt isoforms by siRNA downregulated osteogenic and osteoclastogenic processes, indicating that Akt1 and Akt2 acted synergistically.

Conclusion

LY3023414 can suppress osteogenesis and osteoclastogenesis through inhibition of the PI3K/Akt/GSK3 signalling pathway, which highlights the potential benefits and side effects of LY3023414 for future clinical applications.

Cite this article: *Bone Joint Res* 2021;10(4):237–249.

Keywords: LY3023414, PI3K-Akt signalling pathway, Small interfering RNA, Osteogenesis, Osteoclastogenesis

Article focus

- The function of LY3023414 in bone modelling/remodelling.

Key messages

- LY3023414 inhibits osteogenesis through the phosphatidylinositol 3-kinase (PI3K)/protein kinase B (Akt)/glycogen synthase kinase 3 beta (GSK3β)/β-catenin pathway.
- LY3023414 inhibits osteoclastogenesis through the PI3K/Akt/GSK3β/nuclear factor-activated T cell 1 (NFATc1) pathway, but has little impact on the function of mature osteoclasts.
- Akt isoforms act synergistically, while Akt1 plays a major role.

Correspondence should be sent to Gang Chai; email: chaig1081@sh9hospital.org.cn

doi: 10.1302/2046-3758.104.BJR-2020-0255.R2

Bone Joint Res 2021;10(4):237–249.

Strengths and limitations

- The role of LY3023414 in inhibiting osteogenesis and osteoclastogenesis through the PI3K/Akt/GSK3 signalling pathway was revealed for the first time.
- Small interfering RNA (siRNA) was used to knockdown Akt1 or Akt2 for further validation; this showed that Akt isoforms acted synergistically, while Akt1 played a major role.
- Lack of in vivo data.

Introduction

Bone modelling/remodelling is a dynamic process, which mainly includes osteogenesis (bone formation by osteoblasts) and osteoclastogenesis (osteoclast formation and bone resorption). Abnormalities in bone modelling/remodelling may result in many bone diseases, including osteoporosis[1] and hemifacial microsomia.[2]

LY3023414 is a novel oral dual phosphatidylinositol 3-kinase (PI3K) and mammalian target of rapamycin (mTOR) inhibitor initially designed for tumour therapy.[3] In vitro studies and animal experiments have demonstrated its therapeutic potential for various carcinomas, including oesophageal adenocarcinoma,[4] colorectal cancer,[5] glioma,[6] biliary tract cancer,[7] and skin squamous cell carcinoma.[8] In July 2018, the first human phase I study of LY3023414 was completed in patients with advanced cancer.[9] LY3023414 subsequently showed modest single-agent activity and a manageable safety profile in treating advanced endometrial cancer in a phase II clinical study in March 2020.[10] Nevertheless, little is known about the function of LY3023414 in bone modelling/remodelling.

PI3K/Akt/mTOR is a complex signalling pathway with multiple regulators and effectors. Several studies have confirmed that the PI3K-Akt signalling pathway plays important roles in osteogenesis and osteoclastogenesis. Activation of PI3K/AKT/mTOR can promote osteoblast formation in preosteoblasts and bone mesenchymal stem cells,[11,12] while targeted PI3K/Akt inhibitors, such as LY294002, reduced bone formation both in vivo and in vitro.[13] The PI3K/Akt signalling pathway plays a vital role in the differentiation of osteoclasts, whose inhibition can suppress bone resorption,[14] providing a potential therapeutic target for osteoporosis. In this study, we investigated the effect of LY3023414 on the skeletal system, in order to reveal the potential benefits and side effects for future clinical applications.

Methods

Reagents. Fetal bovine serum (FBS), penicillin/streptomycin, and α-minimum essential medium (α-MEM) were purchased from Thermo Fisher Scientific (USA). The Phospho-Akt (Thr308) primary antibody and the secondary antibodies were purchased from Cell Signaling Technology (USA), while the other primary antibodies were purchased from Abcam (Cambridge, UK) (Table I). Cytokines such as macrophage colony-stimulating factor (MCSF), receptor activator of nuclear factor κB ligand (RANKL), and bone morphogenetic protein-2 (BMP2) were obtained from R&D Systems (USA). The Pan-PI3K inhibitor LY3023414 was purchased from Selleck Chemicals (USA).

Cell culture. Murine bone marrow-derived macrophage cells (BMMs) were freshly isolated from the femora and tibiae of four-week-old C57BL/6 mice, as previously reported.[15] They were cultured in α-MEM supplemented with 10% FBS and 1% penicillin/streptomycin (complete media (CM)), with the addition of 30 ng/ml MCSF (all from Thermo Fisher Scientific). The murine preosteoblast cell line MC3T3-E1 was cultured in CM. All cultures were maintained in a 37°C incubator with 5% CO_2.

Cell viability. An MTS cell proliferation assay (Promega, China) was used to examine the cytotoxicity of LY3023414 (Selleck Chemicals) on BMMs and MC3T3-E1 in accordance with the manufacturer's protocol. Cells seeded on 96-well plates at a density of 1×10^4 cells per well were treated with various concentrations of LY3023414 (10, 20, 40, 80, 160, and 320 nM) for 24, 48, 72, or 96 hours. Control groups were treated with PBS. Thereafter, 10 µl MTS reagent was added to each well and incubated at 37°C for an additional two hours. Absorbance was measured at 492 nm using the absorbance microplate spectrophotometer (Tecan, China). Absorbance readings were normalized to the control group, and the half maximal inhibitory concentration (IC_{50}) was calculated using GraphPad Prism 5 (GraphPad Software, USA).

Osteoclast differentiation and bone resorption. The effect of LY3023414 or Akt gene knockdown on osteoclast differentiation was observed by tartrate-resistant acid phosphatase (TRAP) staining. BMMs were seeded in 96-well plates at 6,000 cells per well (in triplicate) and cultured in CM supplemented with 30 ng/ml of MCSF for 24 hours. For Akt gene knockdown studies, the cells were serum-starved for one hour and then transfected with a mixture of 0.5 µl of Akt small interfering RNA (siRNA) oligos (final concentration of 20 µM) (RiboBio Co, China) or scrambled siRNA control and 0.2 µl Lipo3000 transfection reagent (Thermo Fisher Scientific) in 100 µl serum-free medium for three hours. The transfection mixture was then replaced with CM supplemented with 30 ng/ml MCSF and 100 ng/ml RANKL. For the pan-PI3K inhibitor experiment, BMM cells were treated with various concentrations of LY3023414 (2.5, 5, 10, 20, 40, 80, and 160 nM), 30 ng/ml MCSF, and 100 ng/ml RANKL. Control groups were treated with PBS. Culture media containing MCSF and RANKL were changed every two days until the formation of mature multinucleated osteoclasts in the control groups. Cells were then fixed with 4% paraformaldehyde (Biosharp, China) for 20 minutes, and stained for TRAP activity (Sigma-Aldrich, USA). The number of mature osteoclasts with more than three nuclei and the cell area occupied by these osteoclasts were quantified and scored against the control by ImageJ software (National Institutes of Health, USA).

Table I. Details of the primary antibodies used in this study.

Product name	Company	Catalogue number	Dilution/concentration
Phospho-Akt (Thr308)	CST	#13,038	1/1,000
Anti-pan-Akt	Abcam	ab8805	1/500
Anti-GSK3β (phospho S9)	Abcam	ab131097	1/1,000
Anti-GSK3β	Abcam	ab93926	1/1,000
Anti-beta catenin	Abcam	ab16051	0.25 μg/ml
Anti-Akt1	Abcam	ab233755	1/1,000
Anti-Akt2	Abcam	ab175354	1/1,000
Anti-NFAT2	Abcam	ab25916	2 μg/ml
Anti-GAPDH	Abcam	ab8245	1/2,000

Akt, protein kinase B; Akt1, AKT serine/threonine kinase 1; Akt2, AKT serine/threonine kinase 2; CST, Cell Signaling Technology; GAPDH, glyceraldehyde-3-phosphate dehydrogenase; GSK3β, glycogen synthase kinase 3 beta; NFAT2, nuclear factor of activated T cells 2.

Table II. Details of the primers used in this study.

Gene	Accession number	Forward primer	Reverse primer	Efficiency, %
GAPDH	NM_001289726.1	5′-AGGTCGGTGTGAACGGATTTG-3′	5′-TGTAGACCATGTAGTTGAGGTCA-3′	102
β-actin	NM_007393.5	5′-CCTCTATGCCAACACAGTGC-3′	5′-CCTGCTTGCTGATCCACATC-3′	110
ACP5	NM_001102405.1	5′-CAAAGAGATCGCCAGAACCG-3′	5′-CCTGCTTGCTGATCCACATC-3′	92
CALCR	NM_001042725.1	5′-ACTCCAGTTCTTCAGGCTCC-3′	5′-AGTCAGGGCAGTGCTGATAG-3′	109
CTSK	NM_007802.4	5′-ACTCCAGTCAAGAACCAGGG-3′	5′-TCAGAGTCAATGCCTCCGTT-3′	97
NFATc1	NM_016791.4	5′-CAACGCCCTGACCACCGATAG-3′	5′-GGCTGCCTTCCGTCTCATAGT-3′	104
ALPL	NM_001287172.1	5′-AGAAGTTCGCTATCTGCCTTGCCT-3′	5′-TGGCCAAAGGGCAATAACTAGGGA-3′	108
RUNX2	NM_001146038.2	5′-GACTGTGGTTACCGTCATGGC-3′	5′-ACTTGGTTTTTCATAACAGCGGA-3′	96
Col1a1	NM_007742.4	5′-GCTCCTCTTAGGGGCCACT-3′	5′-CCACGTCTCACCATTGGGG-3′	105
BGLAP	NM_007541.3	5′-TAGCAGACACCATGAGGACCATCT-3′	5′-CCTGCTTGGACATGAAGGCTTTGT-3′	96
SPP1	NM_001204201.1	5′-AGCAAGAAACTCTTCCAAGCAA-3′	5′-GTGAGATTCGTCAGATTCATCCG-3′	102
Akt1	NM_009652.3	5′-CTGCCCTTCTACAACCAGGA-3′	5′-CATACACATCCTGCCACACG-3′	93
Akt2	NM_001110208.2	5′-CTTCGGCAAGGTCATTCTGG-3′	5′-TTGAGGGCTGTAAGGAAGGG-3′	101
Akt3	NM_011785.4	5′-AGCCCAACCTCACAGATTGA-3′	5′-GTGCCACTTCATCCTTTGCA-3′	98

ACP5, acid phosphatase 5, tartrate resistant; Akt, AKT serine/threonine kinase; ALPL, alkaline phosphatase; BGLAP, bone gamma-carboxyglutamate protein; CALCR, calcitonin receptor; Col1a1, collagen type I alpha 1 chain; CTSK, cathepsin K; GAPDH , glyceraldehyde-3-phosphate dehydrogenase; NFATC1, nuclear factor of activated T cells 1; RUNX2, RUNX family transcription factor 2; SPP1, secreted phosphoprotein 1.

For bone resorption, each slice was placed in a single well of a 96-well plate and BMMs (1×10^4 cells/well) were placed on the slice with 30 ng/ml MCSF and 100 ng/ml RANKL. Different concentrations (0, 20, 40, 80 nM) of LY3023414 were added to the culture media on the first or the fifth day, respectively, after RANKL was applied. The media with LY3023414 were changed every two days. The slices were collected eight days after mature osteoclasts were formed for sufficient resorption. Banister brushes were used to wipe off the remaining cells on the slices under water. Bone slices were then imaged by a scanning electron microscope (SEM) (S-4800; Hitachi, Japan) and analyzed by ImageJ software to calculate the absorption area. The 'set scale' function was used to convert the picture size to natural size. Then the 'free-hand selections' function was used for selecting the absorption area according to the colour difference. The 'measure' function was applied to obtain the natural size of bone resorption pits. All the data were presented after normalization with the corresponding control group.

Osteoblast differentiation and staining. MC3T3-E1 cells were maintained in CM for normal growth, and in osteogenic media (10 mM β-glycerophosphate (Sigma-Aldrich), 0.05 mg/ml ascorbic acid (Sigma-Aldrich), 10 nM dexamethasone (Sigma-Aldrich), and 20 ng/ml BMP-2 (R&D System)) for osteoblast differentiation. For Akt gene knockdown studies, the cells (4×10^4 cells/well) were serum-starved for one hour and then transfected with a mixture of 0.5 μl of Akt siRNA oligos (final concentration of 20 μM) or scrambled siRNA control and 0.2 μl Lipo3000 transfection reagent in 100 μl CM for three hours. The transfection mixture was replaced with osteogenic media and the cells were cultured for seven days for assaying the alkaline phosphatase (ALP) activity or for 21 days for the formation of bone nodules. For the pan-PI3K inhibitor experiment, various concentrations of LY3023414 (10, 20, 40, 80, and 160 nM) were directly added to the osteogenic media and the media was changed every three days as needed for a total of seven (ALP activity) or 21 days (bone nodule formation).

At the end of the experimental period, the cells were washed three times with PBS, fixed in 4% paraformaldehyde for 20 minutes at room temperature, and stained with ALP solution or 1% Alizarin Red S (ARS) solution in accordance with the manufacturer's protocol (Beyotime, China). Cells were washed with PBS and digital images were captured using a microscope equipped with 10× and 40× objective lens.

Quantitative real-time polymerase chain reaction. Total cellular RNA was extracted from the cultured cells using a total RNA miniprep kit (Axygen Scientific) according to the manufacturer's protocol. The RNA purity and concentration were assessed using Nanodrop ND-1000 (Thermo Fisher Scientific). Single-stranded complementary DNA (cDNA) was reverse-transcribed from 500 ng total RNA using reverse transcriptase and oligo (dT) primer (PrimeScript RT Master Mix; Takara Biotechnology, Japan) using the following parameters: 37°C for 15 minutes; 85°C for five seconds; and then cooling to 4°C. The primers were designed using Primer 3.0[16–18] by copying the coding sequences (CDS) and setting the product size ranges between 150 bp and 250 bp. The primer sequences are listed in Table II. Quantitative real-time polymerase chain reaction (qRT-PCR) amplification was performed using SYBR Premix Ex Taq (Takara Biotechnology) in an ABI 7500 sequencing detection system (Applied Biosystems, USA) using the following cycling parameters: initial denaturation at 95°C for ten minutes, followed by 40 cycles of ten seconds at 95°C, 15 seconds at 60°C, and ten seconds at 72°C. The comparative $2^{-\Delta\Delta CT}$ method was used to calculate the relative expression of each target gene. We included GAPDH and β-actin as reference genes. As the expression levels of GAPDH were more in the range of those target genes, we used this gene for normalization. The mean cycle threshold (CT) value of target genes was normalized to the CT value of GAPDH to obtain a ΔCT value, which was further normalized to control samples to obtain ΔΔCT. Three independent experiments were conducted, and all samples were performed in triplicates.

Western blot analysis. Total cellular protein extracts were isolated from cultured cells using radio immunoprecipitation assay (RIPA) lysis buffer (50 mM Tris pH 7.5, 150 mM sodium chloride (NaCl), 1% Nonidet P-40, 0.1% sodium dodecyl sulfate (SDS), 1% sodium deoxycholate) (Beyotime, China) supplemented with 1% phenylmethanesulfonyl fluoride (PMSF) and 1% protease inhibitor cocktail (Roche, China). Lysates were cleared by centrifugation at 16,000 ×g for ten minutes at 4°C and the supernatant was collected. The protein concentration was quantified using the BCA protein assay kit (Thermo Fisher Scientific). Extracted proteins were diluted in sodium dodecyl sulfate polyacrylamide gel electrophoresis (SDS-PAGE) loading buffer (Biosharp) and denatured at 95°C for 15 minutes and 300 μg of each protein sample was resolved by 10% SDS-PAGE gel (EpiZyme Scientific, China). Separated proteins were then electroblotted onto polyvinylidene difluoride (PVDF) membranes (Millipore, USA). Following transfer, membranes were blocked with 5% skimmed milk in TBST (tris buffered saline (TBS): 0.05 M Tris, 0.15 M NaCl, pH 7.5%, and 0.2% Tween-20) for one hour and then incubated at 4°C with primary antibodies (Table I) diluted in 1% skimmed milk in TBST overnight. Membranes were washed thrice with TBST and then incubated with anti-mouse or anti-rabbit fluorescent secondary antibodies (according to the primary antibodies used) for one hour at room temperature. After washing thrice with TBST, the membrane was developed using the Odyssey infrared imaging system (LI-COR, USA). The grey value of each blot was measured in the Odyssey V3.0 software (LI-COR) and the relative value of specific protein normalized to GAPDH was calculated.

Statistical analysis. All the experiments were independently repeated three times, and means with standard deviations were used to present the overall data. Firstly, the normality was checked by a Shapiro-Wilk test by means of SPSS v22.0 (IBM, USA). After the normality tests, an analysis of variance was performed for the differences between groups, and independent-samples *t*-test was conducted between the control group and every experimental group in GraphPad Prism 5. Statistical significance was defined as $p < 0.05$.

Results

LY3023414, a pan-PI3K inhibitor, inhibited osteoclastogenesis via the Akt/GSK3β/NFATc1 signalling pathway. The effect of LY3023414 on osteoclast formation and activity was first examined. Low doses of LY3023414 did not affect BMM cell viability, while relatively high doses (75 nM, 150 nM, and 300 nM) resulted in a decline in cell viability (Figure 1a). The IC_{50} was about 384.3 nM at 24 hours, 205.4 nM at 48 hours, 182.3 nM at 72 hours, and 244.3 nM at 96 hours. We then chose 160 nM as the maximum concentration to explore the inhibitory effects of LY3023414 on osteoclast differentiation, in order to ensure that the suppression of osteoclastogenesis by LY3023414 was mainly due to its biological effect and not its toxicity effect. During RANKL-induced osteoclastogenesis, LY3023414 inhibited the formation of TRAP-positive osteoclasts in a dose-dependent manner (Figure 1b). LY3023414 treatment at ≤ 40 nM did not appear to affect the number of osteoclasts formed but decreased the size of the resulting osteoclasts. Only at 160 nM of LY3023414, the number of osteoclasts was markedly reduced to 30% of the control group ($p < 0.01$, independent-samples *t*-test) indicative of the toxic effect of multiple LY3023414 treatments. The effect of LY3023414 on osteoclast size was more apparent at ≥ 40 nM (Figure 1c), with predominantly TRAP-positive mononuclear cells in the 80 nM and 160 nM groups. qRT-PCR analysis of osteoclastic marker genes confirmed the inhibitory effect of LY3023414 on osteoclast differentiation. Gene expressions of acid phosphatase 5, tartrate resistant *(ACP5)*, calcitonin receptor (*CALCR)*, cathepsin K (*CTSK)*, and *NFATc1* were all significantly downregulated

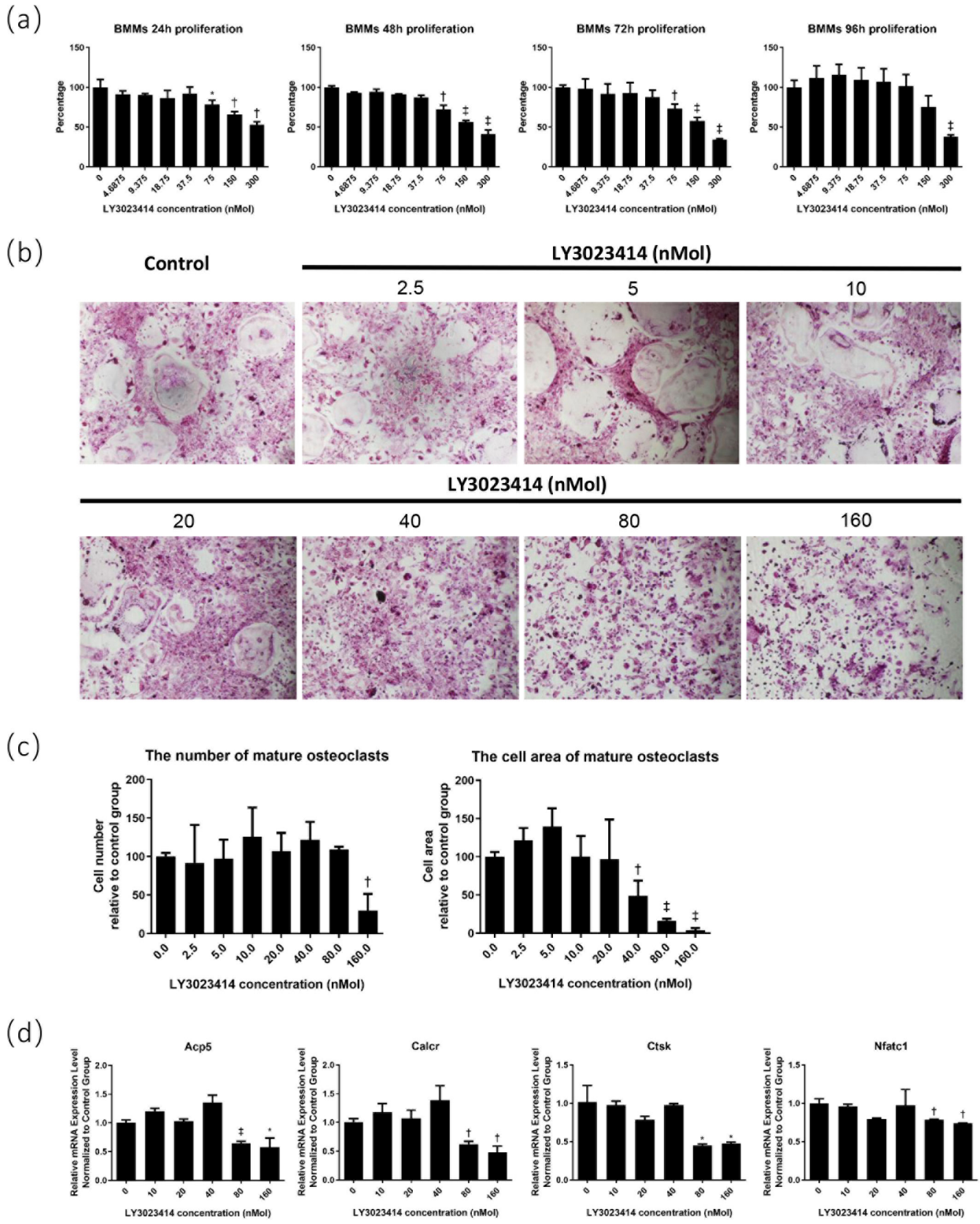

Fig. 1

LY3023414 inhibited osteoclast differentiation. a) LY3023414 inhibited the proliferation of bone marrow-derived macrophage cells (BMMs). Relatively high concentrations of LY3023414 showed apparent toxicity in BMMs. b) The tartrate-resistant acid phosphatase (TRAP) staining (100×) of mature osteoclasts after treatment with different concentrations of LY3023414. High concentrations of LY3023414 suppressed the differentiation of osteoclasts. c) The measurement and analysis of mature osteoclasts in terms of cell number and area. High concentrations of LY3023414 decreased the total area of mature osteoclasts, and the half maximal inhibitory concentration (IC_{50}) of differentiation was about 40 nM. d) Relative messenger RNA (mRNA) expression of osteoclast-specific genes. High concentrations of LY3023414 suppressed the expression levels of acid phosphatase 5, tartrate resistant (Acp5), calcitonin receptor (Calcr), cathepsin K (Ctsk), and nuclear factor of activated T cells 1 (Nfatc1). *$p < 0.05$, †$p < 0.01$, ‡$p < 0.001$.

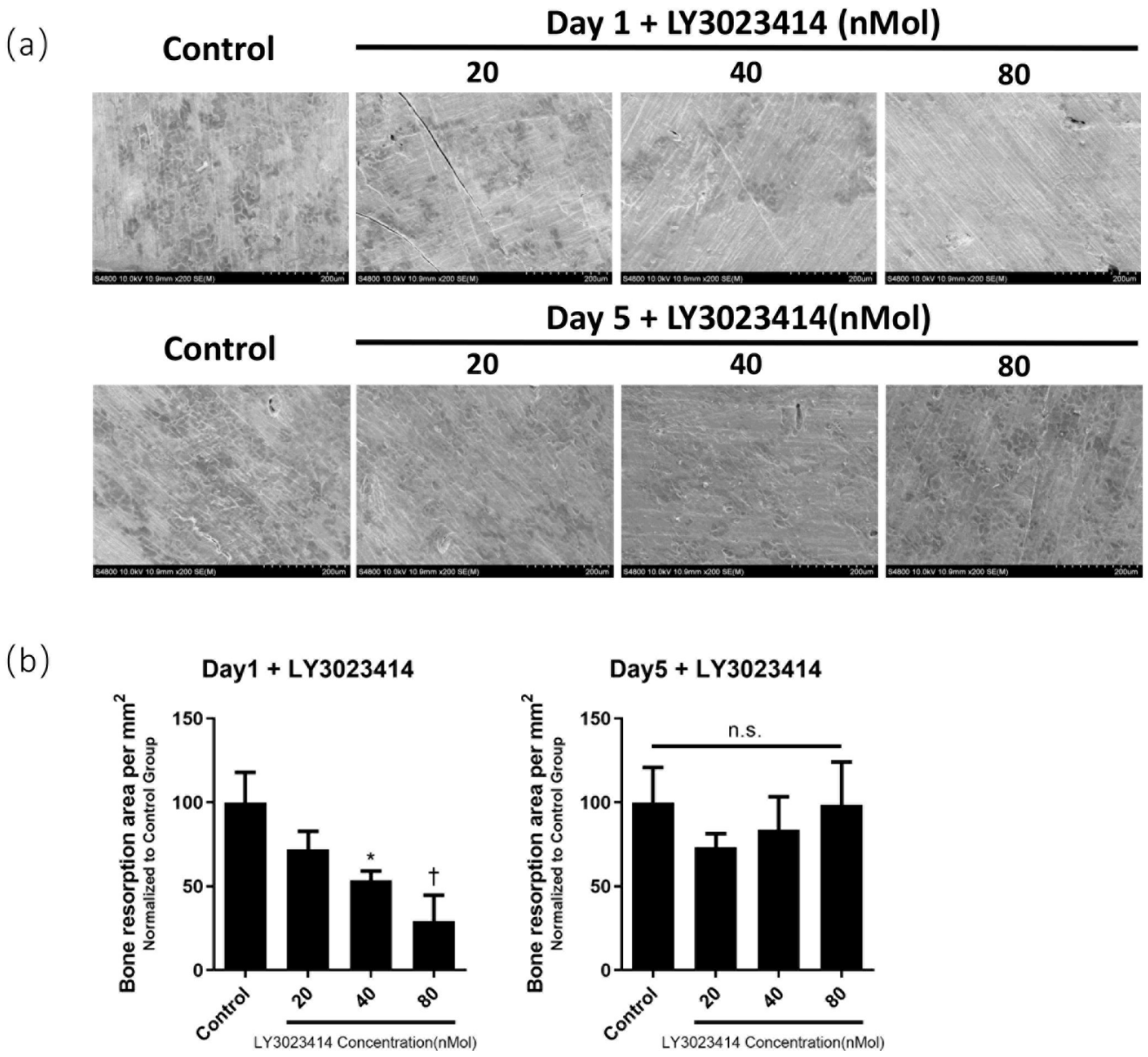

Fig. 2

LY3023414 did not inhibit osteoclasts. a) Scanning electron microscopy (SEM) scans of bone slices. Different concentrations of LY3023414 were added to the osteoclast culture medium on the first day (above) or fifth day (below) supplied with 100 ng/ml receptor activator of nuclear factor κB ligand (RANKL). b) Analysis of bone resorption area per cubic millimetre normalized to the control group. Left: the first-day group. Right: the fifth-day group. *p < 0.05, †p < 0.01, ‡p < 0.001. n.s., no significance.

in the presence of a high dose of LY3023414 (80 nM or 160 nM) (Figure 1d).

Having established that LY3023414 can impair osteoclast formation, we investigated whether inhibition of PI3K/Akt can affect the bone resorptive function of mature osteoclasts. BMM cells were seeded on bovine bone discs and induced to form osteoclasts in the presence of RANKL. Cells treated with indicated concentrations of LY3023414 on the same day as the first dose of RANKL (day 1) showed a dose-dependent reduction in bone resorption. However, cells treated with LY3023414 on day 5 when mature osteoclasts had already formed did not show impairment of bone resorptive activity, indicating that the PI3K/Akt pathway does not play a role in the resorptive process but only during osteoclast formation (Figure 2).

Given that LY3023414 affected osteoclast formation, we then examined the molecular signalling pathway involved in the process. Similar to MCSF stimulation, Akt was phosphorylated within five minutes after RANKL stimulation, peaking at five or ten minutes and stabilizing until 60 minutes. Meanwhile, treatment with LY3023414 significantly reduced RANKL-induced Akt phosphorylation. Moreover, the phosphorylation activation of

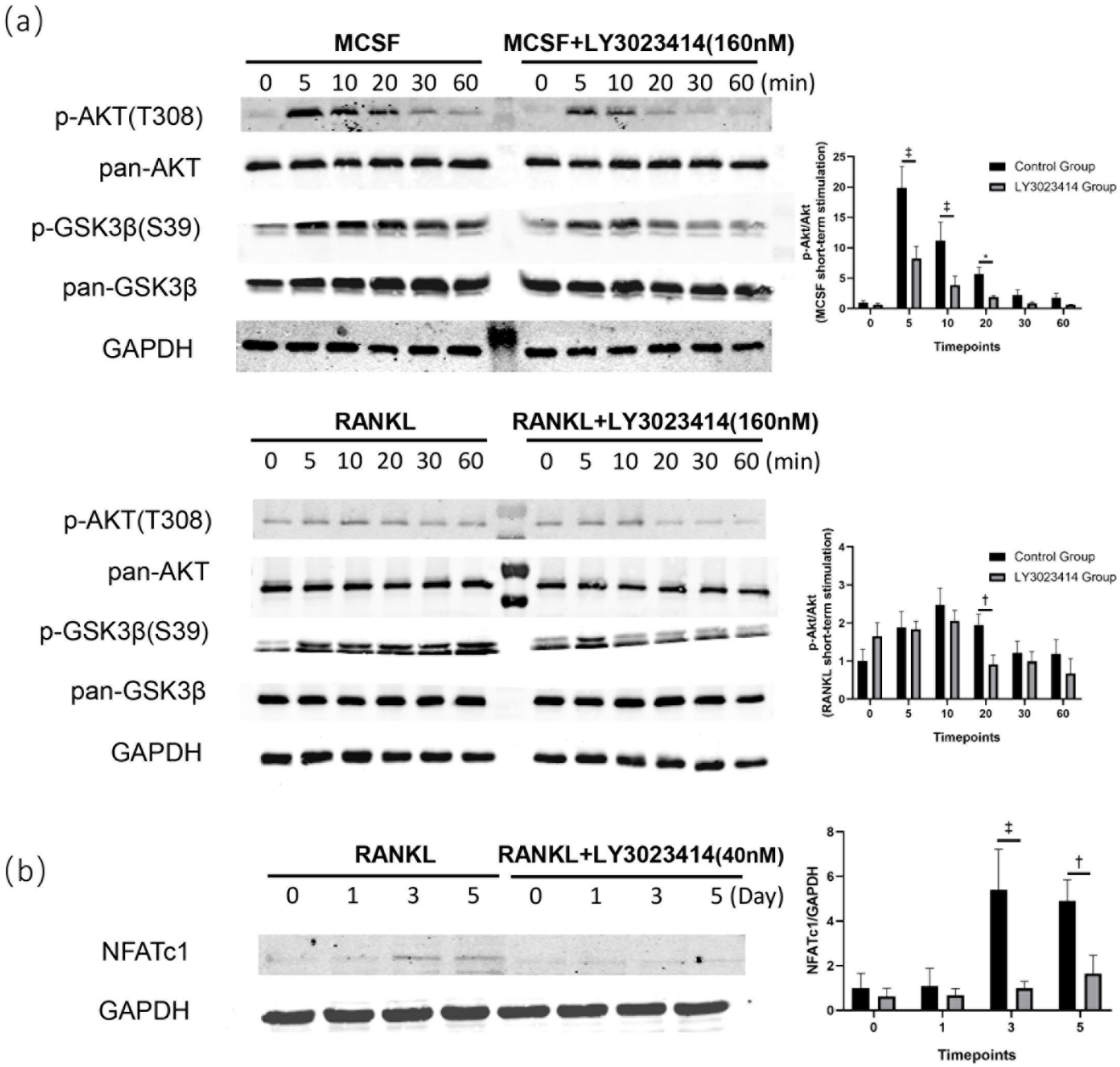

Fig. 3

LY3023414 inhibited osteoclast differentiation through the phosphatidylinositol 3-kinase (PI3K)/protein kinase B (Akt)/glycogen synthase kinase 3 beta (GSK3β)/nuclear factor-activated T cell 1 (NFATc1) signalling pathway. a) The protein expression level of short-term stimulation by macrophage colony-stimulating factor (MCSF) or receptor activator of nuclear factor κB ligand (RANKL) with or without 160 nM LY3023414. LY3023414, as a PI3K inhibitor, suppressed the phosphorylation of Akt. The phosphorylated Akt subsequently suppressed the inactivation of GSK3β. b) The protein expression level of long-term stimulation by MCSF and RANKL with or without 40 nM LY3023414. NFATc1 expression was reduced. *p < 0.05, †p < 0.01, ‡p < 0.001. GAPDH, glyceraldehyde-3-phosphate dehydrogenase.

GSK3β was induced within five minutes of RANKL stimulation, persisting at roughly similar levels throughout the 60-minute time period. Treatment with LY30323414 markedly inhibited the phosphorylation of GSK3β after the initial spike at five minutes (Figure 3a).

NFATc1 is the master and most distal transcriptional regulator that governs osteoclast formation during RANKL stimulation.[19] PI3K-Akt-GSK3β can regulate NFATc1 induction.[20] Thus, we examined the expression of NFATc1 during RANKL-induced osteoclast formation in the presence of LY3023414. As shown in Figure 3b, RANKL induced robust induction of NFATc1 starting around day 3 of osteoclast formation and persisting until day 5, when mature osteoclasts were formed. Meanwhile, treatment with LY3023414 completely abrogated NFATc1 induction, consistent with its inhibitory effect on osteoclast formation.

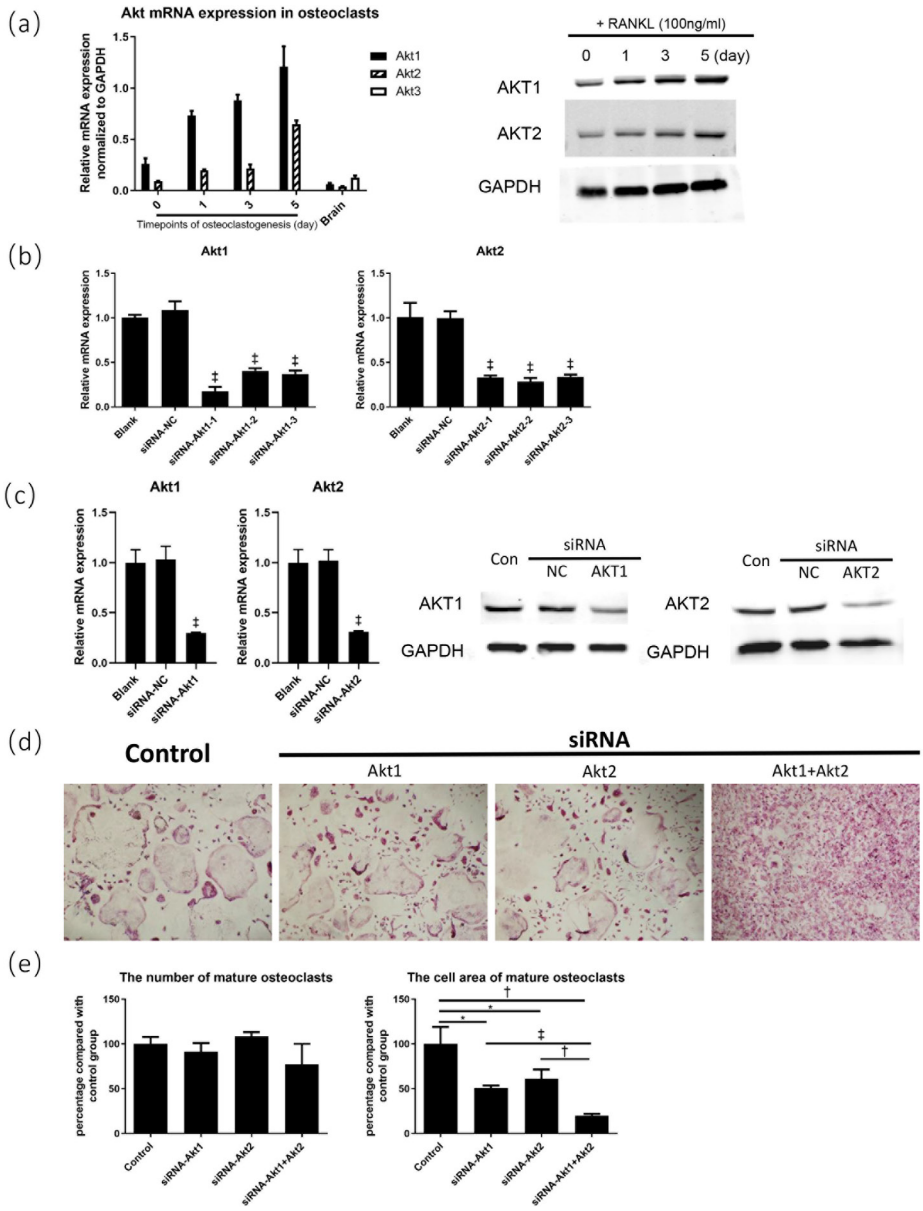

Fig. 4

Silencing of protein kinase B (Akt) inhibited osteoclast differentiation. a) Relative messenger RNA (mRNA) and protein expression levels of Akt isoforms during osteoclastogenesis. b) The performance verification of small interfering RNA (siRNA). Three different siRNA sequences of Akt1 were used, labelled siRNA-Akt1-1, siRNA-Akt1-2, and siRNA-Akt1-3, respectively, and the same labelling method was used for siRNA sequences of Akt2. All three siRNA sequences demonstrated similar effectiveness in suppressing mRNA expression, so they were mixed equivalently in the subsequent study (siRNA-Akt1 represented the mixture of Akt1-1, -2, and -3, same for siRNA-Akt2). c) The performance verification of pooled siRNA. d) The tartrate-resistant acid phosphatase (TRAP) staining (100×) of mature osteoclasts after Akt silencing and receptor activator of nuclear factor κB ligand (RANKL) stimulation. e) The measurement and analysis of mature osteoclasts after Akt silencing. *p < 0.05, †p < 0.01, ‡p < 0.001. Akt1, AKT serine/threonine kinase 1; Akt2, AKT serine/threonine kinase 2; Akt3, AKT serine/threonine kinase 3; Con, control group; GAPDH, glyceraldehyde-3-phosphate dehydrogenase; NC, negative control.

Gene knockdown of Akt1 and Akt2 suppressed osteoclastogenesis. Having established that PI3K plays a role in osteogenesis, we examined whether Akt is involved given that Akt is a key downstream protein of PI3K. We first determined the gene and protein expression of Akt isoforms in BMM precursor cells. During osteoclast formation, both Akt1 and Akt2 genes were expressed in osteoclasts and precursor, with Akt1 showing a more dominant expression level, while Akt3 was absent (Figure 4a).

Next, we determined the gene knockdown efficiency of Akt siRNA oligos. Cells were transfected with three Akt1 or Akt2 siRNA oligos (siRNA-Akt1-1, siRNA-Akt1-2, and siRNA-Akt1-3; siRNA-Akt2-1, siRNA-Akt2-2, and siRNA-Akt2-3) or scrambled siRNA-NC control. As shown in Figure 4b, the transfected siRNA oligos effectively

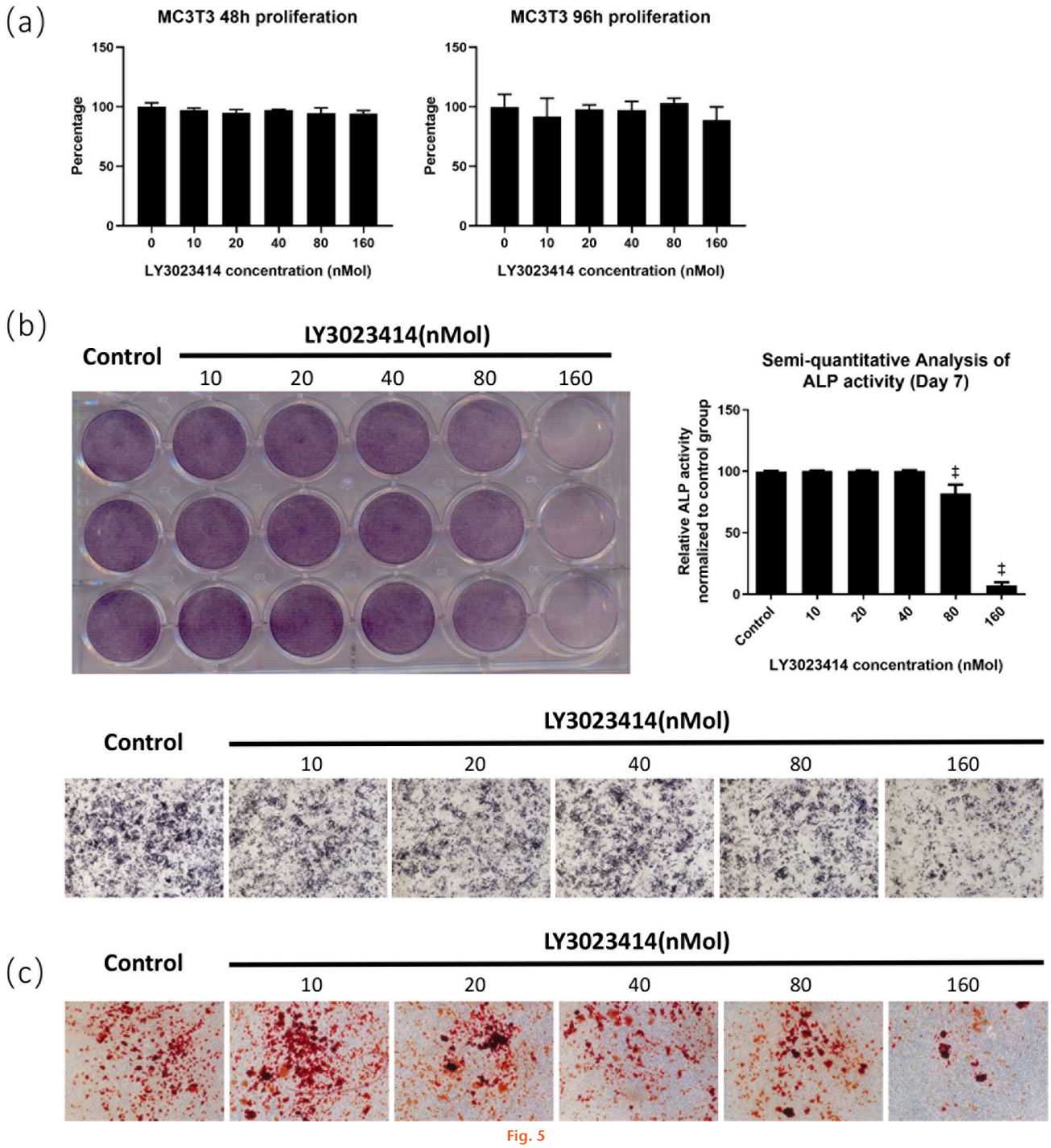

Fig. 5

LY3023414 inhibited osteoblast differentiation. a) LY3023414 demonstrated no toxicity to MC3T3-E1 cell line. b) Alkaline phosphatase (ALP) staining (100×) and semiquantitative analysis of MC3T3-E1 cell line after treatment with different concentrations of LY3023414 and osteogenic induction for seven days. High concentrations (80 nM and 160 nM) of LY3023414 restrained the early stage of osteogenesis. c) Alizarin Red (AR) staining (100×) of MC3T3-E1 cell line after treatment with different concentrations of LY3023414 and osteogenic induction for 21 days. High concentrations of LY3023414, especially the 160 nM group, restrained the late stage of calcification. *p < 0.05, †p < 0.01, ‡p < 0.001.

knocked down Akt1 and Akt2 gene expression, with a > 50% efficiency. Based on these results, we pooled the three Akt1 and Akt2 siRNA oligos, and used the pooled mixture (termed siRNA Akt1 and Akt2 henceforth) for subsequent downstream investigations. The pooled siRNA oligos effectively knocked down the messenger RNA (mRNA) and protein expression of Akt1 and Akt2 in transfected cells. Densitometric analysis of protein bands showed that Akt1 and Akt2 protein expression was down

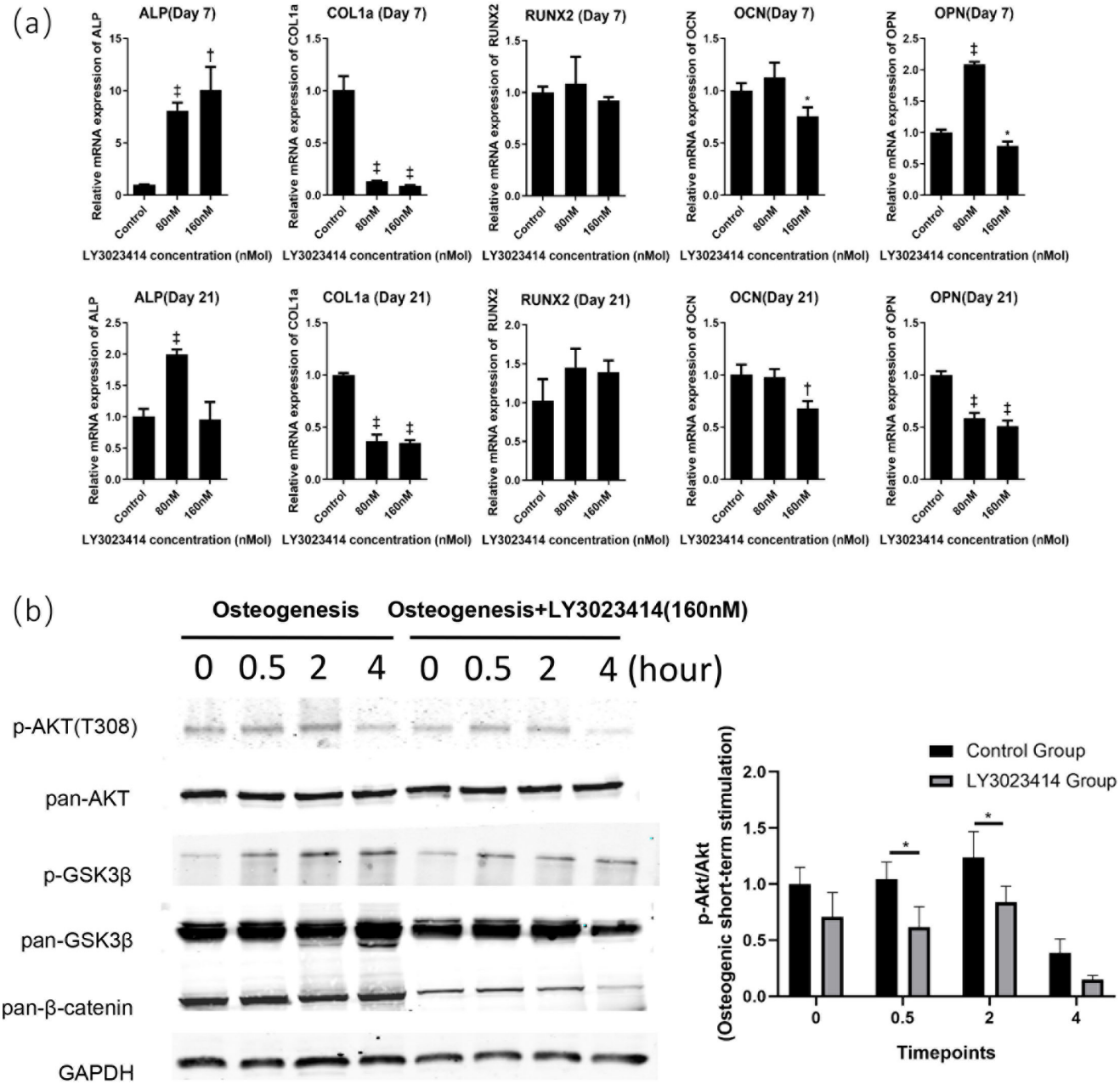

Fig. 6

LY3023414 inhibited osteoblast differentiation through the PI3K/Akt/GSK3β/β-catenin signalling pathway. a) Relative messenger RNA (mRNA) expression of osteoblast-specific genes after LY3023414 treatment and osteogenic induction for seven (above) or 21 days (below). b) The protein expression level of short-term stimulation by osteogenic induction solution with or without 160 nM LY3023414. LY3023414 suppressed the phosphorylation of Akt by inhibiting the activation of Akt. Then the phosphorylated Akt suppressed the inactivation of GSK3β. The phosphorylation of GSK3β suppressed β-catenin. *p < 0.05, †p < 0.01, ‡p < 0.001. ALP, alkaline phosphatase; AKT, protein kinase B; Col1a1, collagen type I alpha 1 chain; GAPDH, glyceraldehyde-3-phosphate dehydrogenase; GSK3β, glycogen synthase kinase 3 beta; OCN, bone gamma-carboxyglutamate protein; OPN, secreted phosphoprotein 1; RUNX2, RUNX family transcription factor 2.

by 35% and 55%, respectively, as compared to cells treated with scrambled siRNA-NC control (Figure 4c).

We next performed Akt1 and Akt2 gene knockdown studies during the process of osteoclast formation (Figure 4d). Knockdown of Akt1+Akt2 did not appear to affect the number of osteoclasts formed, but the size or area occupied by each osteoclast was markedly reduced. Compared with cells transfected with siRNA-NC scramble control, osteoclasts with single Akt1 or Akt2 silencing were 40% to 50% smaller, whereas osteoclasts with both Akt1 and Akt2 silencing were around 80% smaller (Figure 4e). These results suggested that Akt1 and Akt2 may play a role in osteoclast precursor cell fusion.

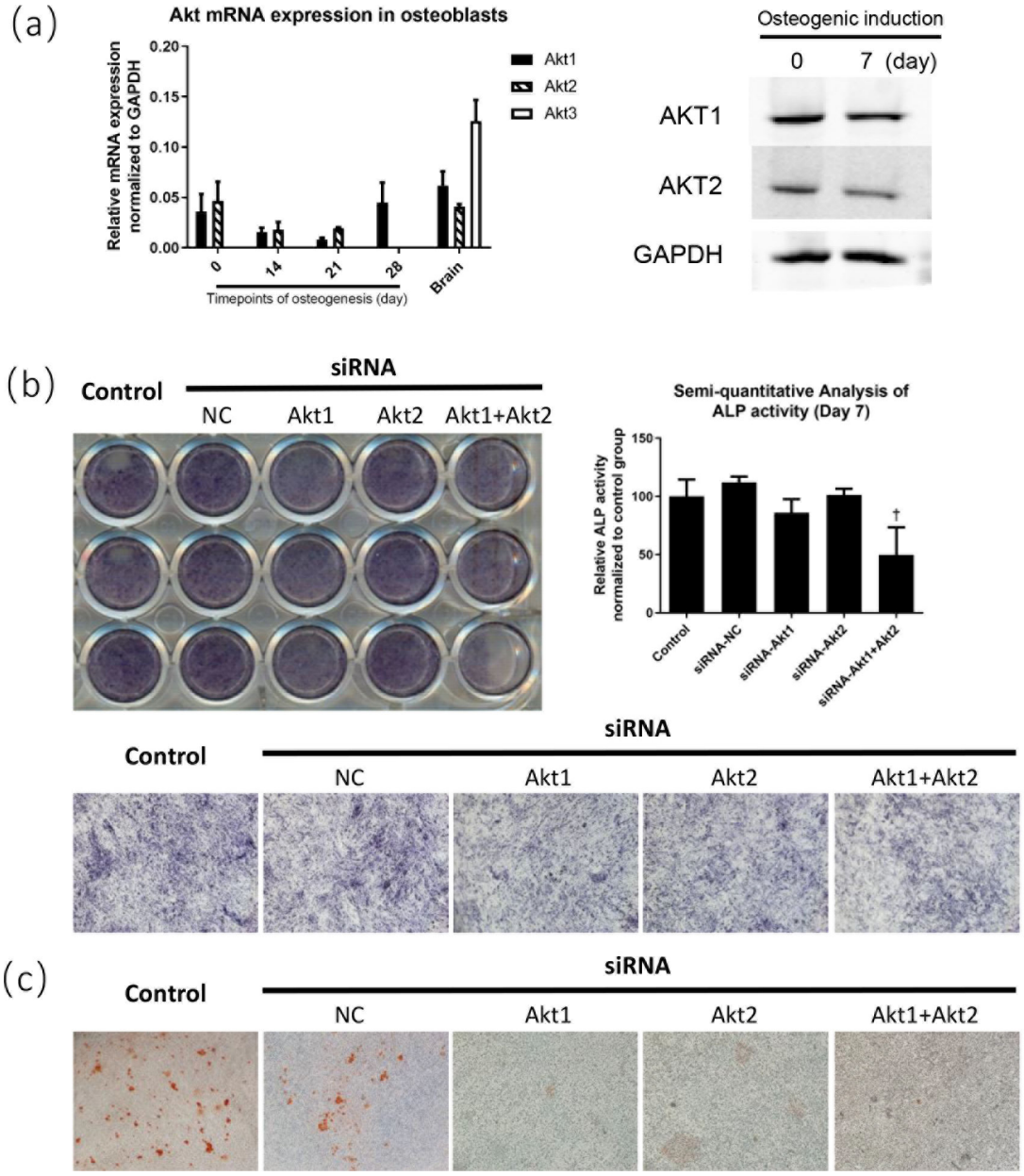

Fig. 7

Silencing of protein kinase B (Akt) inhibited osteoblast differentiation. a) Relative messenger RNA (mRNA) and protein expression levels of Akt isoforms in osteoblasts. b) Alkaline phosphatase (ALP) staining (100×) and semiquantitative analysis of MC3T3-E1 cell line after Akt silencing and osteogenic induction for seven days. c) Alizarin Red (AR) staining (100×) of MC3T3-E1 cell line after Akt silencing and osteogenic induction for 21 days. *p < 0.05, †p < 0.01, ‡p < 0.001. siRNA, small interfering RNA. NC, negative control; Akt1, AKT serine/threonine kinase 1; Akt2, AKT serine/threonine kinase 2; Akt3, AKT serine/threonine kinase 3; GAPDH, glyceraldehyde-3-phosphate dehydrogenase; NC, negative control.

LY3023414, a pan-PI3K inhibitor, inhibited osteogenesis via the Akt/GSK3β/β-catenin signalling pathway. Bone modelling/remodelling is a coupled process, requiring both osteoblastic bone formation and osteoclastic bone resorption. Having established a role for LY3023414 in osteoclastogenesis, we shifted our research focus from the osteoclasts to the osteoblasts.

Using the pan-PI3K inhibitor, LY3023414, we first examined its effect on MC3T3-E1 cell viability. As shown in Figure 5a, treatment of MC3T3-E1 cells with various concentrations of LY3023414 did not affect cell viability. With this result in mind, we conducted osteoblast differentiation assays. Treatment of cells undergoing osteogenic differentiation for seven days resulted in a 20% decrease in ALP activity at 80 nM of LY3023414, and a decrease of > 90% at 160 nM of LY3023414 (Figure 5b). Similarly, mineralization activity and bone nodule formation were

markedly reduced with 160 nM LY3023414 treatment (Figure 5c). Consistent with inhibition of osteoblast differentiation at 160 nM of LY3023414 treatment, expression of osteoblast marker genes such as alkaline phosphatase (ALPL), collagen type I alpha 1 chain (Col1a1), bone gamma-carboxyglutamate protein (BGLAP), and secreted phosphoprotein 1 (SPP1) were mainly downregulated, except for the ALP activity (day 7 for both groups and day 21 for 80 nM group) and OPN activity (day 7 for 80 nM group) (Figure 6a).

We then examined the underlying molecular pathway downstream of PI3K-Akt that is involved in osteogenesis. Using western blot analysis and under short-term osteogenic stimulation (Figure 6b), Akt showed phosphorylation activation within the first two hours, which was significantly reduced at four hours. Activation of phosphorylation of Akt was significantly inhibited by treatment with LY3023414. Downstream of Akt activation, we observed elevated phosphorylation of GSK3β, which was also inhibited in the presence of LY3023414. The level of β-catenin, an important protein during osteogenesis,[21] was markedly reduced in LY3023414-treated cells consistent with inhibition of osteoblast formation.

Akt gene knockdown inhibited early osteogenesis and late-stage calcification. We first determined the mRNA and protein expression of Akt isoforms in the murine pre-osteoblast cell line, MC3T3-E1, using qRT-PCR and western blot analysis, respectively (Figure 7a). Akt1 and Akt2 genes were detected during osteogenesis, while Akt3 gene was not expressed.

We then investigated the effect of Akt1 and/or Akt2 knockdown on osteoblast differentiation. At day 7, knockdown of Akt1 suppressed ALP activity by 29.39%, whereas knockdown of Akt2 suppressed ALP activity by 15.77%. When both Akt1 and Akt2 were knocked down, ALP activity was suppressed by 57.69% (Figure 7b), suggesting that Akt1 and Akt2 synergistically play a role in early osteoblast differentiation.

Late-stage osteoblast differentiation characterized by bone mineralization activity was subsequently examined. As shown by the ARS staining in Figure 7c, bone nodule formation at 21 days of osteogenic differentiation was significantly inhibited following Akt1 and Akt2 knockdown, confirming a role for Akt in osteoblast formation and function.

Discussion

The PI3K/Akt pathway regulates cell proliferation, growth, cell size, metabolism, and motility. This pathway is closely related to many bone diseases such as osteoarthritis,[13] osteosarcoma,[22] and multiple myeloma.[23] Moreover, the PI3K/Akt pathway is commonly activated in human cancers and inhibition of this pathway can lead to regression of human tumours.[24] Bone metastasis, which often accompanies bone destruction, is common in many advanced cancers. LY3023414 is a novel oral PI3K/mTOR dual inhibitor designed for advanced cancer. It has recently completed a phase II clinical trial,[10] which demonstrated modest single-agent activity and a manageable safety profile in treating advanced endometrial cancer. However, little is known about its effect on bone modelling/remodelling, which will help to understand its potential effect on the skeletal system.

In this study, we investigated the role of LY3023414 in bone modelling/remodelling in terms of osteogenesis and osteoclastogenesis. High doses of LY3023414 were cytotoxic, with an IC_{50} of about 160 nM on BMMs. The increased cell death may have, in part, contributed to the reduced number and size of mature osteoclasts, especially at the 160 nM concentration. However, combining the results of obvious decline of cell area of mature osteoclasts in the 40 nM group and the downregulation of specific genes related to osteoclast differentiation, we hypothesized that LY3023414 can pharmacologically inhibit osteoclastogenesis. As for bone resorption, adding the same concentration of LY3023414 at different timepoints caused a significant difference in resorption areas. When the osteoclasts were primarily fused, LY3023414 did not affect the resorption. Thus, LY3023414 mainly affects the process of osteoclast differentiation instead of mature osteoclast functions. Furthermore, this study revealed that LY3023414 suppressed the phosphorylation of Akt, and the phosphorylated Akt suppressed the inactivation of GSK3β, which could directly modulate the activity of NFATc1, a known key modulator in osteoclastogenesis.[25]

Next, the influence of LY3023414 on osteogenesis was explored. Notably, there was an unexpected increase in ALP mRNA expression and OPN activity during osteogenesis. For the ALP activity at day 7, we hypothesized that it may be a compensatory increase. As for the ALP and OPN activity of the 80 nM group at day 21, the underlying reason for these findings was unknown. Nevertheless, according to the staining and changes in other specific genes related to osteogenesis, our data showed that LY3023414 can suppress osteogenesis through the PI3K/Akt/GSK3β/β-catenin signalling pathway, both in the early stage of differentiation and late stage of calcification. GSK3β could influence β-catenin, a terminal protein of the classic Wnt signalling pathway[26] that plays an important role in osteoblast differentiation.[27]

Thereafter, siRNA was used for verification and further investigation. Akt is the key downstream protein of PI3K, and has three isoforms: Akt1, Akt2, and Akt3. Akt1 and Akt2 are widely expressed in all tissues at varying levels, whereas expression of Akt3 is limited to the brain and testis.[28] The silencing of Akt isoforms in MC3T3-E1 or BMMs, irrespective of Akt1 or Akt2, could also inhibit both osteogenesis and osteoclastogenesis. Compared with Akt2, Akt1 silencing was more effective in conformity to its distribution,[29] and the combined Akt1+Akt2 silencing was even more effective.

As a preliminary study investigating the effect of LY3023414 on bone modelling/remodelling, this study had several limitations. First, although this study clarified

the function of LY3023414 on osteogenesis and osteoclastogenesis through the PI3K/Akt/GSK3 signalling pathway, more detailed mechanisms were not probed. There are many interactions between the PI3K/Akt signalling pathway and Smad signalling, MAPK signalling, and in particular the JNK/p38 signalling pathway.[30,31] Moreover, we did not check the function of LY3023414 on bone modelling/remodelling in vivo. The combined effect of suppressing both osteogenesis and osteoclastogenesis requires further study. Whether this drug interacts with other signalling pathways needs to be clarified.

Collectively, the results of this study provided evidence that LY3023414 could inhibit both osteogenesis and osteoclastogenesis. It may help to understand the potential benefits or side effects of this drug for future clinical applications. LY3023414 may have a potential protective effect on the bone since it can inhibit osteoclastogenesis and bone resorption. Meanwhile, LY3023414 also has a certain inhibitory effect on osteogenesis. Special attention should be paid to bone mass during the medication, especially in postmenopausal women with advanced endometrial cancer.

References

1. **Ensrud KE**, **Crandall CJ**. Osteoporosis. *Ann Intern Med*. 2017;167(3):ITC17–ITC32.
2. **Vong A**, **Funamura J**. Multidisciplinary management of oculo-auriculo-vertebral spectrum. *Curr Opin Otolaryngol Head Neck Surg*. 2018;26(4):234–241.
3. **Smith MC**, **Mader MM**, **Cook JA**, **et al**. Characterization of LY3023414, a novel PI3K/mTOR dual inhibitor eliciting transient target modulation to impede tumor growth. *Mol Cancer Ther*. 2016;15(10):2344–2356.
4. **Zaidi AH**, **Kosovec JE**, **Matsui D**, **et al**. Pi3K/mTOR dual inhibitor, LY3023414, demonstrates potent antitumor efficacy against esophageal adenocarcinoma in a rat model. *Ann Surg*. 2017;266(1):91–98.
5. **Foley TM**, **Payne SN**, **Pasch CA**, **et al**. Dual PI3K/mTOR Inhibition in Colorectal Cancers with *APC* and *PIK3CA* Mutations. *Mol Cancer Res*. 2017;15(3):317–327.
6. **Zheng L**, **Li H**, **Mo Y**, **Qi G**, **Liu B**, **Zhao J**. Autophagy inhibition sensitizes LY3023414-induced anti-glioma cell activity *in vitro* and *in vivo*. *Oncotarget*. 2017;8(58):98964–98973.
7. **Sakamoto Y**, **Yamagishi S**, **Tanizawa Y**, **Tajimi M**, **Okusaka T**, **Ojima H**. Pi3K-mTOR pathway identified as a potential therapeutic target in biliary tract cancer using a newly established patient-derived cell panel assay. *Jpn J Clin Oncol*. 2018;48(4):396–399.
8. **Zou Y**, **Ge M**, **Wang X**. Targeting PI3K-AKT-mTOR by LY3023414 inhibits human skin squamous cell carcinoma cell growth in vitro and in vivo. *Biochem Biophys Res Commun*. 2017;490(2):385–392.
9. **Bendell JC**, **Varghese AM**, **Hyman DM**, **et al**. A first-in-human phase 1 study of LY3023414, an oral PI3K/mTOR dual inhibitor, in patients with advanced cancer. *Clin Cancer Res*. 2018;24(14):3253–3262.
10. **Rubinstein MM**, **Hyman DM**, **Caird I**, **et al**. Phase 2 study of LY3023414 in patients with advanced endometrial cancer harboring activating mutations in the PI3K pathway. *Cancer*. 2020;126(6):1274–1282.
11. **Mukherjee A**, **Rotwein P**. Akt promotes BMP2-mediated osteoblast differentiation and bone development. *J Cell Sci*. 2009;122(Pt 5):716–726.
12. **Xie X**, **Liu M**, **Meng Q**. Angelica polysaccharide promotes proliferation and osteoblast differentiation of mesenchymal stem cells by regulation of long non-coding RNA H19: an animal study. *Bone Joint Res*. 2019;8(7):323–332.
13. **Sun K**, **Luo J**, **Guo J**, **Yao X**, **Jing X**, **Guo F**. The PI3K/Akt/mTOR signaling pathway in osteoarthritis: a narrative review. *Osteoarthritis Cartilage*. 2020;28(4):400–409.
14. **Moon JB**, **Kim JH**, **Kim K**, **et al**. Akt induces osteoclast differentiation through regulating the GSK3β/NFATc1 signaling cascade. *J Immunol*. 2012;188(1):163–169.
15. **Kobayashi K**, **Takahashi N**, **Jimi E**, **et al**. Tumor necrosis factor alpha stimulates osteoclast differentiation by a mechanism independent of the ODF/RANKL-RANK interaction. *J Exp Med*. 2000;191(2):275–286.
16. **Untergasser A**, **Cutcutache I**, **Koressaar T**, **et al**. Primer3--new capabilities and interfaces. *Nucleic Acids Res*. 2012;40(15):e115.
17. **Koressaar T**, **Remm M**. Enhancements and modifications of primer design program Primer3. *Bioinformatics*. 2007;23(10):1289–1291.
18. **Kõressaar T**, **Lepamets M**, **Kaplinski L**, **Raime K**, **Andreson R**, **Remm M**. Primer3_masker: integrating masking of template sequence with primer design software. *Bioinformatics*. 2018;34(11):1937–1938.
19. **Takayanagi H**, **Kim S**, **Koga T**, **et al**. Induction and activation of the transcription factor NFATc1 (NFAT2) integrate RANKL signaling in terminal differentiation of osteoclasts. *Dev Cell*. 2002;3(6):889–901.
20. **Wu M**, **Chen W**, **Lu Y**, **Zhu G**, **Hao L**, **Li Y-P**. Gα13 negatively controls osteoclastogenesis through inhibition of the Akt-GSK3β-NFATc1 signalling pathway. *Nat Commun*. 2017;8:13700.
21. **Pan J-X**, **Xiong L**, **Zhao K**, **et al**. Yap promotes osteogenesis and suppresses adipogenic differentiation by regulating β-catenin signaling. *Bone Res*. 2018;6:18.
22. **Zhang J**, **Yu X-H**, **Yan Y-G**, **Wang C**, **Wang W-J**. Pi3K/Akt signaling in osteosarcoma. *Clin Chim Acta*. 2015;444:182–192.
23. **Ramakrishnan V**, **Kumar S**. Pi3K/Akt/mTOR pathway in multiple myeloma: from basic biology to clinical promise. *Leuk Lymphoma*. 2018;59(11):2524–2534.
24. **Alzahrani AS**. Pi3K/Akt/mTOR inhibitors in cancer: at the bench and bedside. *Semin Cancer Biol*. 2019;59:125–132.
25. **Chen W**, **Zhu G**, **Tang J**, **Zhou H-D**, **Li Y-P**. C/Ebpα controls osteoclast terminal differentiation, activation, function, and postnatal bone homeostasis through direct regulation of NFATc1. *J Pathol*. 2018;244(3):271–282.
26. **Lerner UH**, **Ohlsson C**. The Wnt system: background and its role in bone. *J Intern Med*. 2015;277(6):630–649.
27. **Jacobsen CM**, **Schwartz MA**, **Roberts HJ**, **et al**. Enhanced Wnt signaling improves bone mass and strength, but not brittleness, in the Col1a1(+/mov13) mouse model of type I Osteogenesis Imperfecta. *Bone*. 2016;90:127–132.
28. **Cohen MM**, **Jr**. The Akt genes and their roles in various disorders. *Am J Med Genet A*. 2013;161A(12):2931–2937.
29. **Hers I**, **Vincent EE**, **Tavaré JM**. Akt signalling in health and disease. *Cell Signal*. 2011;23(10):1515–1527.
30. **Biver E**, **Thouverey C**, **Magne D**, **Caverzasio J**. Crosstalk between tyrosine kinase receptors, GSK3 and BMP2 signaling during osteoblastic differentiation of human mesenchymal stem cells. *Mol Cell Endocrinol*. 2014;382(1):120–130.
31. **Rodríguez-Carballo E**, **Gámez B**, **Ventura F**. P38 MAPK signaling in osteoblast differentiation. *Front Cell Dev Biol*. 2016;4(21):40.

Author information:
- X. Chen, MD, Postgraduate
- W. Chen, MD, Postgraduate
- Z. M. Aung, MD, Surgeon
- W. Han, MM, Postgraduate
- Y. Zhang, MD, Senior doctor
- G. Chai, MD, Senior doctor

Department of Plastic and Reconstructive Surgery, Shanghai Ninth People's Hospital, Shanghai Jiao Tong University School of Medicine, Shanghai, China.

Author contributions:
- X. Chen: Conducted the experiments, Analyzed the data, Drafted the manuscript.
- W. Chen: Conducted the experiments, Drafted the manuscript.
- Z. M. Aung: Prepared the primary cell culture.
- W. Han: Analyzed the data.
- Y. Zhang: Reviewed and revised the manuscript.
- G. Chai: Conceptualized the study, Reviewed and revised the manuscript.

- X. Chen and W. Chen contributed equally to this work.

Funding statement:
- This work was supported by the National Natural Science Foundation of China (81741012); Clinical Research Program of 9th People's Hospital, Shanghai Jiao Tong University School of Medicine (JYLJ031). No benefits in any form have been received or will be received from a commercial party related directly or indirectly to the subject of this article.

Ethical review statement:
- This study was approved by the Ethics Committee of Shanghai Ninth People's Hospital, Shanghai Jiao Tong University School of Medicine.